Available online at www.sciencedirect.com
SCIENCE DIRECT®
Journal of Sound and Vibration 288 (2005) 729–749
JOURNAL OF SOUND AND VIBRATION
www.elsevier.com/locate/jsvi

Towards a diffusion model of acoustic energy flow in large undamped structures

Nicholas L. Wolff, Richard L. Weaver*

Department of Theoretical and Applied Mechanics, University of Illinois at Urbana–Champaign, 216 Talbot Lab, 104 S. Wright Street, Urbana, Illinois 61801, USA

Accepted 5 July 2005
Available online 31 August 2005

Abstract

It is shown that energy transport parameters for vibrations in a complex structure may be extracted from the kind of data that might be obtained from limited and cost effective direct numerical simulations (DNS). A diffusion model is proposed which promises to avoid the requirement of statistical energy analysis (SEA)-like substructuring. The model is successfully fit to simulated data with an underlying nature which is unambiguously diffusive, as opposed to DNS data where the underlying nature is in question. The data is constructed with noise that mimics the sorts of fluctuations expected in practice. The algorithm's robustness depends heavily on the number of adjustable parameters.

1. Introduction

It has long been appreciated that direct numerical simulations (DNS) of the dynamics of large structural acoustic systems, though possible in principle, can be impractical due to high computational demands. Meeting such demands can be particularly challenging if fine resolution is required in either space or time, or if the solution at late times is required. Moreover, such a solution is necessarily sensitive to the fine details of the structure. A DNS to the dynamics of one

*Corresponding author. Fax: +1 217 244 5707.
E-mail address: r-weaver@uiuc.edu (R.L. Weaver).

0022-460X/$ - see front matter © 2005 Published by Elsevier Ltd.
doi:10.1016/j.jsv.2005.07.013

Nomenclature

$\mathbf{d}$, $\mathbf{D}$	$N \times N$ symmetric matrix representing smooth underlying energy flow in an SEA description, $R \times R$ symmetric matrix representing energy flow in a measurable quantity description
$\mathbf{G}(t)$	Green's function
$\mathbf{g}$	$R \times N$ matrix of (site specific frequency dependent) gains to translate from the SEA description to the measurables description
$\mathbf{h}$, $\mathbf{H}$	$N \times N$ diagonal matrix containing mode counts for an SEA description, $R \times R$ diagonal matrix for a measurable quantity description
n, N	substructure index, total number of substructures
r, R	receiver index, total number of receivers
N_t	total number of times
$\mathbf{v}^i$, $\mathbf{V}^i$	eigenvectors associated with the ith eigenvalue in the SEA energy density ($N \times 1$) and measurables ($R \times 1$) descriptions, respectively
λ_i, Λ_i	ith eigenvalue in the measurables and SEA descriptions, respectively
$\hat{\pi}$, $\hat{\Pi}$	$N \times 1$ forcing in the SEA description, $R \times 1$ forcing in the measurables description
σ	fractional standard deviation of noise added evolution of energy density
$\psi(t)$, $\Psi(t)$	$N \times 1$ vector of local underlying SEA energy densities, $R \times 1$ vector of mean square signals

structure, then, is of little value when considering the dynamics of another structure that differs in its details. Investigators have therefore been seeking efficient statistical descriptions of responses.

Statistical energy analysis (SEA) [1–5] is one approach to obtaining such estimates. In conventional SEA steady-state energy densities are predicted for bandlimited responses in the presence of dissipation. SEA models require a partition of the system into weakly coupled substructures; they also require modal densities and dissipation estimates for each substructure, and estimates of the coefficients that determine energy flow between them. Direct finite element numerical simulations [5–9] have been used to estimate the parameters of an SEA model, though more commonly they are estimated from analytic models or experimental observations. Recent years have seen extensions of SEA to the time domain [10,11] and development of some hybrid methods [12].

Weaver [13] considered the problem of estimating bandlimited mean-square late-time responses in large undamped systems. An undamped model is used to seek improved models of energy transport in complex systems. The analysis of undamped systems is simpler than that of more realistic systems; however, the undamped case does contain sufficient relevant and subtle issues to recommend its study in connection to energy flow. The method was similar to SEA and transient SEA[1] in that it introduced concepts related to modal density and equipartition, but different in that there was no substructuring. The regime of applicability of the procedures in this paper is the same as that in Ref. [13]. Namely, it is similar to that of SEA, but more general in that it promises to apply to systems that do not admit substructuring. The late time mean-square response at a receiver with spatial distribution $\mathbf{r}$ (a normalized vector of generalized displacements) to a narrow band source $B(t)$ with spatial distribution $\mathbf{s}$ (a normalized vector of generalized forces) was

[1]Henceforth, we do not distinguish transient SEA from SEA, as they have the same logical basis and information content.

estimated by

$$\Psi_{rs,B}(t=\infty)=\frac{E_{r,B}E_{s,B}}{2\pi^3 f_c^2 D(2\pi f_c)\int B^2(t)\,\mathrm{d}t}, \tag{1}$$

where

$$E_{s,B}=\int_0^{T_B} B(t)\left[\frac{\mathrm{d}}{\mathrm{d}t}\int_0^t (\mathbf{s}^{\mathrm{T}}\mathbf{G}(t-\tau)\mathbf{s})B(\tau)\,\mathrm{d}\tau\right]\mathrm{d}t \tag{2}$$

has the interpretation of the work done by the source $B(t)$ with spatial distribution $\mathbf{s}$. Reciprocity is evident. In the above, f_c is the center frequency of the frequency band, $D(\omega)$ is the global modal density, and T_B is the duration of the source B. The matrix $\mathbf{G}(t)$ is the Green's function. Diagonal elements of $\mathbf{G}(t)$ for each receiver and source of interest are required. However, such knowledge is needed for only short times, and thus may be obtained by a DNS with only modest computational burden. Thus late time mean square responses are estimated efficiently in terms of local impedances and global modal density.

Eq. (1) can be thought of as a product of admittances. We note that Eq. (2) can be rewritten [13] as

$$E_{s,B}=-\frac{1}{\pi}\int_0^\infty \omega|\tilde{B}(\omega)|^2\Im\tilde{\mathbf{G}}_{ss}(\omega)\,\mathrm{d}\omega, \tag{3}$$

where the tilde represents Fourier transform. The imaginary part of the admittance (admittance = inverse of impedance Z) is $\Im(1/Z)=\omega\Im\tilde{\mathbf{G}}(\omega)$. Henceforth $E_{s,B}$ will loosely be referred to as the admittance at site s.

This previous work showed that early time responses determine (frequency-smoothed) late-time energies. It did not address energy flow at moderate times. But early time responses also describe a degree of transport which, if observed in a DNS, could be extrapolated to later times. The statistical energy ansatz supposes that energy transport is diffusive. If the parameters of that diffusion model can be taken from the behavior of short-time-scale DNS, it may be that energy flow can be extrapolated to long times using the diffusion parameters apparent at early times. This is the goal of a project for which this paper is a part. We note, though, that a diffusion model need not be identical to SEA. In particular, like Ref. [13], it need not require substructuring. Diffusion models can be stated in different ways, and one such is described in Section 2 and found to be related to SEA.

In the present paper the problem of estimating the parameters of a diffusion model from data that might be obtained from a short time DNS is considered and an attempt to delineate the requirements of such a fit is made. An undamped model is used in order to simplify the issues. Further, we take data not from a DNS of the wave equation, but from the exact solution of supposed underlying diffusion, with statistical fluctuations characteristic of a DNS. The aim of this paper is not to compare DNS data with diffusion, but rather to develop procedures to fit a diffusion model to data that is unequivocally diffusion-like. The program here uses time domain data like Gregory and Keltie [14], but may be contrasted with their work in which experimental data is used to estimate SEA parameters. Sections 3 and 4 contain a discussion of the generation of this artificial data. The results of fits to data from a two room system and from a three room

system are presented here. It is found that accurate fits can be obtained using data from only early times. In Section 5, we conclude and indicate directions for future work.

2. Two descriptions of diffusion

In order to approximately describe the complicated dynamics of a vibrational system, we adopt a diffusion-like model for energy flow. First, the form this model takes in terms of measurable quantities such as mean square response and mean square forcing (the quantities used in Ref. [13]) is described. To the end of extracting the diffusion parameters of this measurables model, we assume that the structure does admit a division into substructures. Thus there is an exact correspondence, in this case, to SEA.

2.1. Description of the model in terms of measured quantities

We begin with an assumed diffusion-like energy flow equation governing the slow evolution of band-limited energy. The description is in terms of slowly time-varying mean square displacement Ψ at each of R receivers avoids the need for substructuring, so it can be applied to a dynamical system without first having to substructure it in order receivers and in terms of mean square forcings $\hat{\Pi}$ (which may act through some of those receivers). In the absence of dissipation, the equation takes the form

$$\mathbf{H}\frac{\partial}{\partial t}\Psi(t) = \hat{\Pi}(t) - \mathbf{D}\Psi(t), \tag{4}$$

where $\mathbf{H}$ and $\mathbf{D}$ are $R \times R$, Ψ contains the mean square displacements and is $R \times 1$, and $\hat{\Pi}$ represents average band-limited force squared and is also $R \times 1$. The total number of receivers (potential sources) is denoted by R. These are the measurable quantities discussed in Ref. [13]. Our ansatz is somewhat more general than SEA, albeit still diffusive. SEA is one special case of our theory. The proposed approach makes no assumptions about substructures: it can be applied to a dynamical system without the need to substructure it in order to define modal energy density in a substructure and coupling loss factors between substructures, and to systems that do not admit discrete substructures. Whether or not it is valid to apply a diffusion-like model at all is another matter, and a long standing question within SEA.

We imagine having generated that data Ψ and $\hat{\Pi}$ by DNS over short times. Thus it is inexpensive to employ a large number, R, of receivers; however, each source site requires a separate DNS of the impulse response of the system, so use of multiple sources is more expensive. It is desired to determine the diffusion parameters.

The matrix $\mathbf{H}$ must be diagonal in order that a forcing at one location does not instantaneously result in a response at another location. Any such energy transport may be restricted to be a consequence of possibly large off diagonal elements in the construction of $\mathbf{D}$. The matrix $\mathbf{D}$ must be symmetric as argued by reciprocity.[2] In the Laplace transform domain, one finds that

[2]Reciprocity between force and displacement implies reciprocity between mean square force $\hat{\Pi}$ and mean square displacement Ψ.

the solution is

$$\Psi(s) = (\mathbf{D} + s\mathbf{H})^{-1}\hat{\Pi}(s). \tag{5}$$

The matrix $(\mathbf{D} + s\mathbf{H})^{-1}$ must be symmetric for all s implying that both $\mathbf{H}$ and $\mathbf{D}$ must be symmetric.

In discussing the solution to Eq. (4), consider the generalized eigenvalue problem

$$\mathbf{DU} = \Lambda\mathbf{HU}, \tag{6}$$

with eigenpairs $(\Lambda_r, \mathbf{V}^r)$, $r = 1, 2, \ldots, R$. In the absence of dissipation, the first eigenvalue is trivial, that is $\Lambda_1 = 0$. The eigenvectors are orthogonal and normalized:

$$\mathbf{V}^{r\mathrm{T}}\mathbf{H}\mathbf{V}^q = \delta_{rq}, \tag{7a}$$

$$\mathbf{V}^{r\mathrm{T}}\mathbf{D}\mathbf{V}^q = \Lambda_r\delta_{rq}, \tag{7b}$$

where the superscript T denotes transpose.

Consider the "impulsive" band-limited forcing described by

$$\hat{\Pi}(t) = \Pi\delta(t) \tag{8}$$

along with quiescent initial conditions. One finds the solution to Eq. (4) to be

$$\Psi(t) = \sum_{r=1}^{R} \mathbf{V}^r\mathbf{V}^{r\mathrm{T}}\Pi \mathrm{e}^{-\Lambda_r t}\Theta(t), \tag{9}$$

where $\Theta(t)$ is the Heaviside function. This solution is just an expansion in eigenvectors, each multiplied by a decaying exponential. As summarized above in Section 1, previous work by Weaver [13] shows that the mode associated with the trivial eigenvalue $\Lambda_1 = 0$ can be estimated accurately and directly from a short time[3] DNS. This mode is constructed via Eq. (1) as follows:

$$\mathbf{V}_r^1 = \frac{E_{r,B}}{\sqrt{2\pi^3 f_c^2 D(2\pi f_c)}}. \tag{10}$$

Knowing this for any site r requires a short time DNS with a source at r.

2.2. Description of the model in terms of energy density

As in SEA [1], we can also attempt to describe the diffusion in terms of energy flow between several (N) substructures. The governing equation is much the same as Eq. (4) above. It is, in the absence of dissipation,

$$\mathbf{h}\frac{\partial}{\partial t}\psi(t) = \hat{\pi}(t) - \mathbf{d}\psi(t), \tag{11}$$

where $\mathbf{h}$ and $\mathbf{d}$ are $N \times N$, ψ contains the modal energy densities (energy per mode) in some frequency band Δf in each substructure and is $N \times 1$, and $\hat{\pi}$ contains power, the rate at which

[3]A length of time comparable to the inverse of the desired frequency resolution.

energy is deposited into each substructure, and is also $N \times 1$. The number of substructures is denoted by N.

The matrix $\mathbf{h}$ is diagonal and contains the known mode counts, so these are not parameters to be extracted. Because SEA assumes equipartition of energy among the various modes across each substructure in a frequency band Δf, this definition implies that the left-hand side of Eq. (11) can be interpreted as the time rate of change of total energy in each substructure. Through this definition $\mathbf{d}$ must be symmetric. This follows from setting the net energy flux from substructure b to substructure a (equal to $\mathbf{d}_{ab}\psi_b - \mathbf{d}_{ba}\psi_a$) to zero when $\psi_a = \psi_b$. Alternatively, one argues that the net flux is proportional (only) to the difference $\psi_a - \psi_b$.

In Ref. [11], the $\mathbf{h}$ matrix was is assumed to be the identity matrix, and $\mathbf{d}$ was non-symmetric. That formulation may be obtained from this by changing the dependent variable from the modal energy densities used here to total substructure energies used in Ref. [11] and elsewhere.

Again, there is a set of eigenpairs $(\lambda_n, \mathbf{v}^n)$, $n = 1, 2, \ldots, N$ associated with Eq. (11). In the absence of dissipation, the first eigenvalue is trivial, that is $\lambda_1 = 0$. The eigenvectors are orthogonal and normalized:

$$\mathbf{v}^{n\mathrm{T}}\mathbf{h}\mathbf{v}^q = \delta_{nq}, \tag{12a}$$

$$\mathbf{v}^{n\mathrm{T}}\mathbf{d}\mathbf{v}^q = \lambda_n\delta_{nq}. \tag{12b}$$

The solution of Eq. (11) in the case of impulsive loading $\hat{\pi}(t) = \pi\delta(t)$ and quiescent initial conditions follows in exactly the same way as for Eq. (4),

$$\psi(t) = \sum_{n=1}^{N} \mathbf{v}^n\mathbf{v}^{n\mathrm{T}}\pi \mathrm{e}^{-\lambda_n t}\Theta(t). \tag{13}$$

Equipartition across the entire structure at late times implies that the first eigenvector is

$$\mathbf{v}_n^1 = 1/\sqrt{\mathrm{tr}(\mathbf{h})} \tag{14}$$

for all n. This is normalized (Eq. (12a)).

2.2.1. Connection to the measured quantity description

If a substructured description is valid (and one can imagine systems for which it is not), there must be a connection between the measured quantities Ψ and the substructures' energies ψ. We define $\mathbf{g}$, a typically non-square ($R \geqslant N$) matrix of local frequency-dependant transducer functions and sensitivities (henceforth simply called gains) such that

$$\Psi(t) = \mathbf{g}\psi(t). \tag{15}$$

Elements of $\mathbf{g}$ are the sensitivities of the response of the transducer to the local dynamics multiplied by the sensitivity of the local dynamics to the local geometrical details of the structure, i.e. the admittances.

That there is a unique mapping in Eq. (15) between substructure energy and mean square displacement at sites within the substructure is a consequence of the diffuse field assumption—that total energy is statistically equivalent to energy density samples. Cases in which the mapping is non-unique follow from failures of the diffuse field assumption, and/or poor substructuring.

Presumably, if the structures of the SEA description are geometrically separated, $\mathbf{g}$ is especially simple. That is, $\mathbf{g}_{rn}$ is non-zero if and only if receiver r is physically located in substructure n. This implies that each row of $\mathbf{g}$ has only one non-trivial element. Unless otherwise noted in the sections to follow, such a $\mathbf{g}$ is assumed, implying that the systems are such that

1. There is a strict substructuring such that the mean square response at any given receiver is directly proportional to the energy density in (only) that substructure.
2. It is known in which substructure each receiver is located.

These requirements will ultimately need to be relaxed if the methods are to be applied to systems which do not admit subtructuring. We will eventually want to consider fully populated $\mathbf{g}$ matrices such that the response at any given receiver site may be some weighted average of the energy density in different substructures. In particular one can think of at least two counterexamples to the above assumption of the special case $\mathbf{g}$.

1. One might imagine two large rooms with a small window providing the coupling between the two rooms. Presumably, if a receiver is located close to the window, the response at that site would be a weighted average of the local energy density in each room.
2. One can consider diffusion across a statistically uniform structure. Multiple scattering of waves in such systems is often described by diffusion [15,16]. The concept of substructures in this case becomes problematic, and one would expect an SEA description to fail and the need for $\mathbf{g}$ to vanish in this case.

We proceed to derive the relationship between the eigenvalues and eigenvectors of the measured quantities description and the energy density description. Substituting Eqs. (9) and (13) into Eq. (15), we have

$$\Psi(t) = \sum_{r=1}^{R} \mathbf{V}^r \mathbf{V}^{r\mathrm{T}} \Pi \mathrm{e}^{-\Lambda_r t} \Theta(t) = \mathbf{g} \sum_{n=1}^{N} \mathbf{v}^n \mathbf{v}^{n\mathrm{T}} \pi \mathrm{e}^{-\lambda_n t} \Theta(t). \tag{16}$$

Thus it is inferred

$$\mathbf{V}^r = \mathbf{g}\mathbf{v}^n \delta_{rn} \quad \text{for } r \leqslant N, \tag{17a}$$

$$\mathbf{g}^{\mathrm{T}} \Pi = \pi, \tag{17b}$$

$$\Lambda_r = \begin{cases} \lambda_n \delta_{rn} & \text{for } r \leqslant N, \\ \infty & \text{otherwise.} \end{cases} \tag{17c}$$

establishing the relationships between the eigenvectors, power inputs, and eigenvalues in the measurables description and the energy density description. In particular, the small eigenvalues ($r \leqslant N$) in the measured quantities description are the same as those in the energy density description while the large eigenvalues ($r > N$) are at least approximated to be infinite. Note that to obtain the eigenvectors in the measured space, one left multiplies the corresponding eigenvectors in the physical space with the $\mathbf{g}$ matrix in identically the same way as one obtains the

Ψ vector from the ψ vector. Also note that Eq. (17a) applied to $r = 1$ allows us to solve for the elements of $\mathbf{g}$, at least for the strict substructuring $\mathbf{g}$, since $\mathbf{V}^1$ and $\mathbf{v}^1$ are completely known.

We can consider the orthogonality of the eigenvectors in the SEA description and in the measured data description. We have by substituting Eq. (17a) into Eq. (7a)

$$\mathbf{V}^{r\mathrm{T}}\mathbf{H}\mathbf{V}^{q} = \mathbf{v}^{r\mathrm{T}}\mathbf{g}^{\mathrm{T}}\mathbf{H}\mathbf{g}\mathbf{v}^{q} = \delta_{rq} \tag{18}$$

as well as from Eq. (12a)

$$\mathbf{v}^{p\mathrm{T}}\mathbf{h}\mathbf{v}^{s} = \delta_{ps}. \tag{19}$$

Therefore,

$$\mathbf{g}^{\mathrm{T}}\mathbf{H}\mathbf{g} = \mathbf{h}. \tag{20}$$

This appears to be $N(N+1)/2$ equations (orthogonality conditions) in R unknowns (diagonal elements of $\mathbf{H}$). If, however, only strict substructuring is considered, inspection of Eq. (20) reveals that the equations associated with the off diagonal elements of $\mathbf{h}$ are automatically satisfied. Then this is N equations in R unknowns, a completely determined system if there is one and only one receiver in each substructure. If there is more than one receiver in any substructure, this means there is some freedom in choosing how to distribute the $\mathbf{H}$'s among the receiver sites in that substructure.

3. Case study I: two room system

Our long range desire is to be able to fit short-time DNS measured data to a diffusion model in order to be able to predict transport dynamics over longer times. Towards this end we here generate data artificially and attempt to fit it to equations like Eq. (16). The parameters of diffusion (i.e. λ's, $\mathbf{v}$'s, and $\mathbf{g}$) will be recovered by minimizing a χ^2 quantity by adjusting the diffusion parameters, explained below.

We consider two simple case studies, each of the strict substructuring class which maps well onto SEA. One has two substructures; another has three. For these studies mode counts are taken as known and admittances (i.e. $\mathbf{V}^1$) are taken as known by a procedure like that of Weaver [13] for sites with a source. Forcing Π would be known in a DNS simulation, so these are not parameters to be extracted by the program.

3.1. Description of data

The data to be fit is constructed first by evaluating the SEA solution Eq. (13) in a simple two substructure system. With a view towards application to data gleaned from a DNS, with inevitable stochastic fluctuations and local variations in sensitivities, we then add noise and multiply by arbitrarily specified receiver gains $\mathbf{g}$. Noise is constructed such that it has fixed[4]

[4]This is typical. Moreover the fractional standard deviation is $\sigma = 1/\sqrt{\Delta f \Delta t}$ in real DNS applications or measurements where Δf is the bandwidth in a DNS or measurement, and Δt is the duration of the time window over which energies are averaged [17–20].

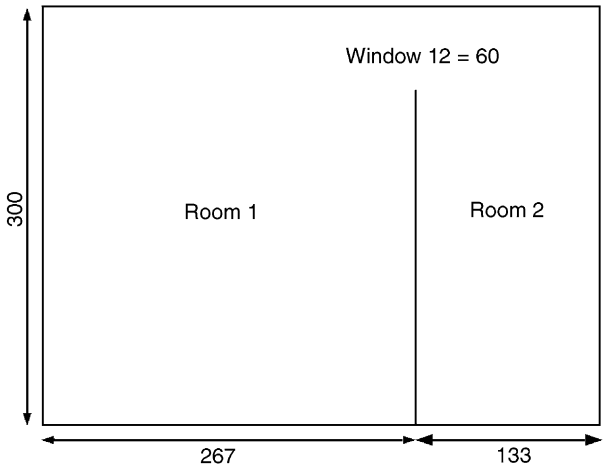

Fig. 1. Geometry of the two room system described in Section 3. The window coupling the two rooms is $l_{12} = 60$ units wide. Units of length are referenced to an arbitrary microscopic length scale L, equal to $\frac{1}{300}$ of the room width.

fractional standard deviation σ, and it is constructed independently at each r, t. The details are in Appendix A.

Our system in the first case study is equivalent to that used to describe room acoustics in the structure pictured in Fig. 1 of size 400×300 with a partition along its width. The partition has a window of length $l_{12} = 0.20 \times 300 = 60$ allowing energy to flow between the two (two dimensional) rooms. In practice, this window has to be small for "weak-coupling" but larger than a few wavelengths to avoid localization. Therefore, the parameters of Eq. (11) with mode counts being taken in the usual way (see, e.g. Ref. [21]) are the following:

$$\mathbf{h}_n = \frac{2\pi f}{c^2}(\text{area}_n)\Delta f,$$

$$\mathbf{d} = \frac{cl_{12}}{\pi}\begin{bmatrix} 1 & -1 \\ -1 & 1 \end{bmatrix} \times \frac{\text{number of modes}}{\text{area}},$$

where c is the velocity of the waves, f is the center frequency of the frequency band, and Δf is the band width. The velocity and frequency are taken here as unity and the bandwidth is taken as $1/2\pi$ for the purposes of our artificial simulation. The $\{\psi\}$'s thus represent modal energy density, plotted in Fig. 2. These parameters result in a first non-trivial eigenvalue of $\lambda_2 = 7.2 \times 10^{-4}$. The gains in the $\mathbf{g}$ matrix were taken from a set of uniformly distributed numbers $[\frac{1}{2}, 2]$.

We considered four data sets each with a total of 20 receivers, 10 in each room, and took data from two "experiments" corresponding to sources in each of the two rooms. Data was examined out to one-tenth of a decay time, i.e. $t_{\max} = 139$, and 20 data points were constructed for each receiver at evenly spaced times. Fractional fluctuations from the mean energy density were different in each data set and taken to be $\sigma = 0\%$, $\sigma = 15\%$, $\sigma = 30\%$, and $\sigma = 50\%$.

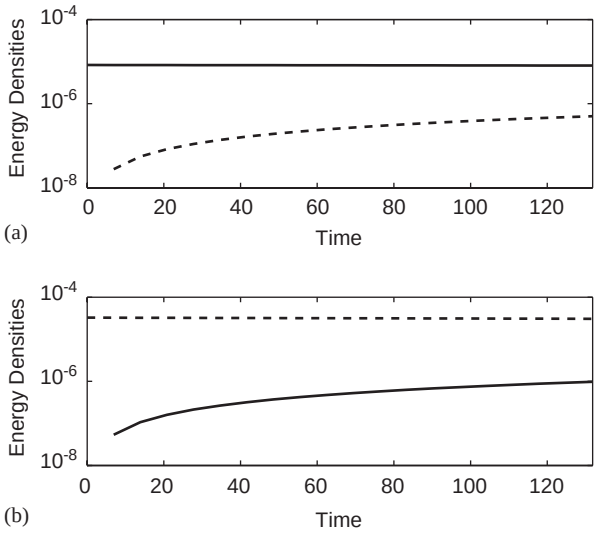

Fig. 2. The evolution of energy density in each of the two rooms for the period analyzed in Section 3. ————, response in room 1; – – – – – –, response in room 2. Time is measured in units of L/c. The eigenvalues (in units of c/L) are $\lambda_1 = 0$ and $\lambda_2 = 7.2 \times 10^{-4}$. The eigenvectors are $\mathbf{v}^1 = \{2.9; 2.9\} \times 10^{-3}$ and $\mathbf{v}^2 = \{2.0; -4.1\} \times 10^{-3}$. Total time considered was $\frac{1}{10}(1/\lambda_2)$: (a) a single source in room 1; (b) a single source in room 2.

3.2. Fitting procedure

We seek to fit the functional form in Eq. (16)

$$\Psi(t) = \mathbf{g} \sum_{n=1}^{N} \mathbf{v}^n \mathbf{v}^{n\mathrm{T}} \pi \mathrm{e}^{-\lambda_n t} \tag{21}$$

to the artificial data. Since $\mathbf{v}^1$ is completely known (Eq. (14)) and $\mathbf{V}^1$ is taken as known for the two source locations, elements in the rows of the $\mathbf{g}$ matrix corresponding to the source locations can be calculated by Eq. (17a) (but remain unknown for its other 18 elements). One can calculate $\mathbf{v}^2$ using the two remaining orthogonality conditions:

$$\mathbf{v}_1^1 \mathbf{h}_1 \mathbf{v}_1^2 + \mathbf{v}_2^1 \mathbf{h}_2 \mathbf{v}_2^2 = 0, \tag{22a}$$

$$\mathbf{v}_1^2 \mathbf{h}_1 \mathbf{v}_1^2 + \mathbf{v}_2^2 \mathbf{h}_2 \mathbf{v}_2^2 = 1. \tag{22b}$$

Solving directly results in

$$\mathbf{v}_1^2 = \frac{\mathbf{v}_2^1 \mathbf{h}_2}{\alpha}, \tag{23a}$$

$$\mathbf{v}_2^2 = -\frac{\mathbf{v}_1^1 \mathbf{h}_1}{\alpha}, \tag{23b}$$

where

$$\alpha = \sqrt{(\mathbf{v}_2^1\mathbf{h}_2)^2\mathbf{h}_1 + (\mathbf{v}_1^1\mathbf{h}_1)^2\mathbf{h}_2}, \tag{24}$$

so that $\mathbf{v}^2$ is completely known entirely from the specified parameters; the data is not needed to find $\mathbf{v}^2$. The use of the mapping of Eq. (15) may seem to restrict the method only to systems that admit substructuring. However, the substructuring is exploited to reduce the number of fit parameters in the nonlinear fit algorithm that is used and to map directly onto SEA. This apparent need for substructuring could be relaxed simply by fitting all of the gains, or, equivalently, fitting all of the elements of the eigenvectors $\mathbf{V}$.

The remaining quantities must be fit by minimizing a χ^2 quantity. The formula for χ^2 can take a few different forms, e.g.:

$$\chi_a^2 = \frac{\sum_t \sum_{r=1}^{R} \sum_{s=1}^{S} [[\mathbf{G}_{rs}(t) - \Psi_{rs}(t)]^2 / [\sigma \mathbf{G}_{rs}(t)]^2]}{N_t RS - \text{dof}}, \tag{25a}$$

$$\chi^2 = \frac{\sum_t \sum_{r=1}^{R} \sum_{s=1}^{S} [\log \mathbf{G}_{rs}(t) - \log \Psi_{rs}(t)]^2}{\sigma^2 (N_t RS - \text{dof})}, \tag{25b}$$

where dof is the number of fitting parameters and σ^2 (defined by Eq. (30)) is the fractional variance of the signal about the local underlying mean and is identical for every value of $\Psi_{rs}(t)$. The above two forms are nominally equivalent, such that a good fit should have $\chi^2 \sim$ unity. Eq. (25b) is particularly convenient because of the relatively simple form of the expression.

The remainder of the fitting process consists of letting a nonlinear least square fitting algorithm search the degrees of freedom to minimize χ^2. The algorithm used is a MATLAB implementation of a "large scale: trust-region reflexive Newton" method [22]. For this problem the logarithm of the data (i.e. in Eq. (25b)) is fit to the log of the functional form of Eq. (21) with the adjusted parameters being the eigenvalue λ_2 and the 18 elements in the rows of $\mathbf{g}$ not associated with sources.

The above procedure may be contrasted with that of Gregory and Keltie [14]. They use an eigensystem realization algorithm (ERA) [23], a linearized fit algorithm, to obtain estimates for the eigenvalues. However, ERA does not perform well in our experience with our time-limited data. ERA seems to weight all data equally without normalizing by the mean value, i.e. using a non-weighted χ^2 like

$$\chi_{nw}^2 = \frac{\sum_t \sum_{r=1}^{R} \sum_{s=1}^{S} [\mathbf{G}_{rs}(t) - \Psi_{rs}(t)]^2}{N_t RS - \text{dof}}. \tag{26}$$

If $\mathbf{G}$ has large dynamic range and fluctuates with a fixed fractional standard deviations σ, Eq. (26) is inappropriate.

3.3. Results

We evaluate the performance of our algorithm by scrutinizing the best fits to the eigenvalues and the value of χ^2 associated with the best fit. The best fits to the eigenvalues are plotted in Fig. 3 for different number of receivers in each room considered and different noise levels. The fit

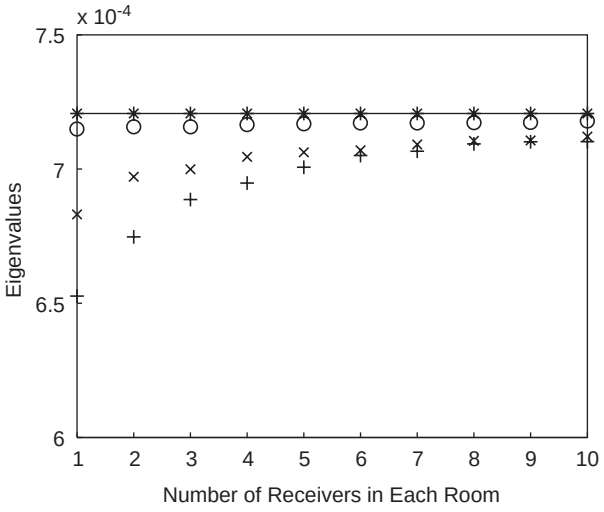

Fig. 3. The best fit to λ_2 for the two room system for various numbers of receivers in each room and noise levels. ————, correct value(s); $*\ *$, $\sigma = 0\%$; $o\ o$, $\sigma = 15\%$; $\times\ \times$, $\sigma = 30\%$; $+\ +$, $\sigma = 50\%$. The fit is good even with a small number of receivers and large noise amplitude.

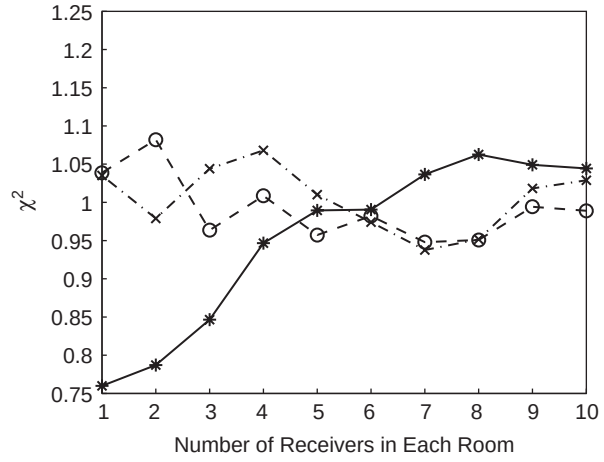

Fig. 4. The χ^2 value after the fit for various numbers of receivers and noise amplitudes. $-*-*-$, $\sigma = 15\%$; $-o-o-$, $\sigma = 30\%$; $-\times-\times-$, $\sigma = 50\%$. This value fluctuates randomly about unity as it should. The value of χ^2 shows that the fit is good even for a small number of receivers and large noise amplitudes.

algorithm is seen to find the best fit to the decay time regardless of the number of receivers in the experiment or the noise amplitude.

As shown in Fig. 4, the best fit value of chi-square was evaluated. It fluctuates about unity as it should. The best fit to data from a receiver in each of the substructures is plotted along with the data in Fig. 5. The overall fit was to all 10 receivers in both substructures.

The fitting algorithm in this two room case is successful and robust.

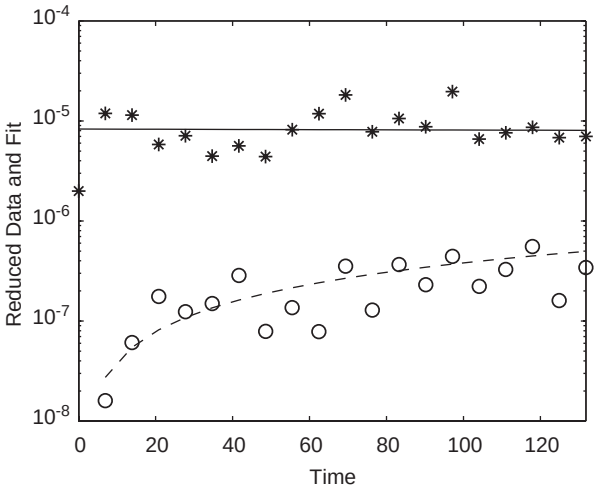

Fig. 5. An example of the actual fit to the data with noise fluctuations $\sigma = 50\%$. $*\,*$, data from a site in room 1; ————, fit to data from room 1; $\circ\,\circ$, data from a site in room 2; – – – – –, fit to data from room 2. The source in room 1. The overall fit was to data from 10 receivers in each room.

4. Case study 2: three room system with partial coupling

Finally, we extend the class of problems we are considering slightly to a three room system with no coupling between rooms one and three (i.e., three rooms "in a row").

4.1. Description of the data

We consider a structure pictured in Fig. 6 of size 400×300, this time with two partitions dividing it into three rooms. The partitions have windows of lengths $l_{12} = 0.20 \times 300 = 60$ and $l_{23} = 0.25 \times 300 = 75$ allowing energy to flow between the rooms. Therefore, the parameters of Eq. (11) with mode counts (with $l_{13} = 0$) approximated by

$$\mathbf{h}_n = \frac{2\pi f^2}{c^2}(\text{area}_i)\Delta f,$$

$$\mathbf{d} = \frac{c}{\pi}\begin{bmatrix} l_{12}+l_{13} & -l_{12} & -l_{13} \\ -l_{12} & l_{12}+l_{23} & -l_{23} \\ -l_{13} & -l_{23} & l_{13}+l_{23} \end{bmatrix} \times \frac{\text{number of modes}}{\text{area}},$$

where c is the velocity of the waves, f is the center frequency of the frequency band, and Δf is the band width. The velocity and frequency are taken here to be unity and the bandwidth is taken to be $1/2\pi$ for the purposes of the artificial simulations. $\{\psi\}$'s thus represent modal energy density, plotted in Fig. 7. These parameters result in a first non-trivial eigenvalue of about 4.7×10^{-4} and second non-trivial eigenvalue of about 22.5×10^{-4}. The gains in the $\mathbf{g}$ matrix were taken from a set of uniformly distributed numbers $[\frac{1}{2}, 2]$.

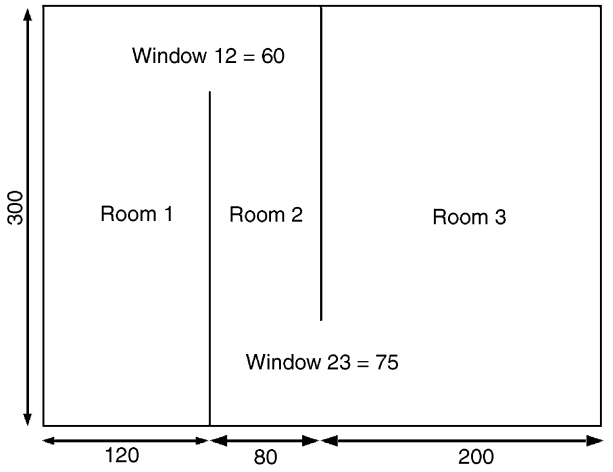

Fig. 6. Geometry of the system described in Section 4. The window coupling rooms 1 and 2 is $l_{12} = 60$ units wide and the window coupling rooms 2 and 3 is $l_{23} = 75$ units wide.

We consider three data sets each with a total of 30 receivers, 10 in each room, and took data from three "experiments" corresponding to sources in each of the three rooms. Data was examined out to one-half of the longer decay time, i.e. $t_{\max} = 1060$, and 20 data points were constructed for each receiver at evenly spaced times. Fractional fluctuations from the mean energy density were different in each data set and taken to be $\sigma = 0$, 15, and 30%.

4.2. Fitting procedure

We seek to fit the form of Eq. (21) with $N = 3$ to the data. Since $\mathbf{v}^1$ is completely known and $\mathbf{V}^1$ is taken to be known for the three source locations considered, those associated elements of $\mathbf{g}$ can be calculated completely by Eq. (20). One element of one of the higher eigenvectors in the energy description must be adjusted in the fitting procedure. All that remains is to calculate the remaining elements of $\mathbf{v}^2$ and $\mathbf{v}^3$ using the five remaining orthogonality conditions. The solution can be found in Appendix B.

The eigenvalues, λ_2 and λ_3; one element in the eigenvectors, $\mathbf{v}_1^2$; and the 27 elements of $\mathbf{g}$ not already taken to be known are the adjusted parameters.

4.3. Results

We evaluate the performance of our algorithm by scrutinizing the best fits to the eigenvalues and the value of χ^2 associated with the best fit. The best fits to the eigenvalues are plotted in Fig. 8 for different number of receivers in each room and different noise levels. The fit algorithm does find the best fit to the decay times if enough receivers are considered.

If more receivers are considered in the data set (not shown), the fit fails because of the higher number of parameters (gains) that need to be adjusted in the fit procedure. The correct global minimum χ^2 was not found; instead some other local minimum was found. This may be surprising

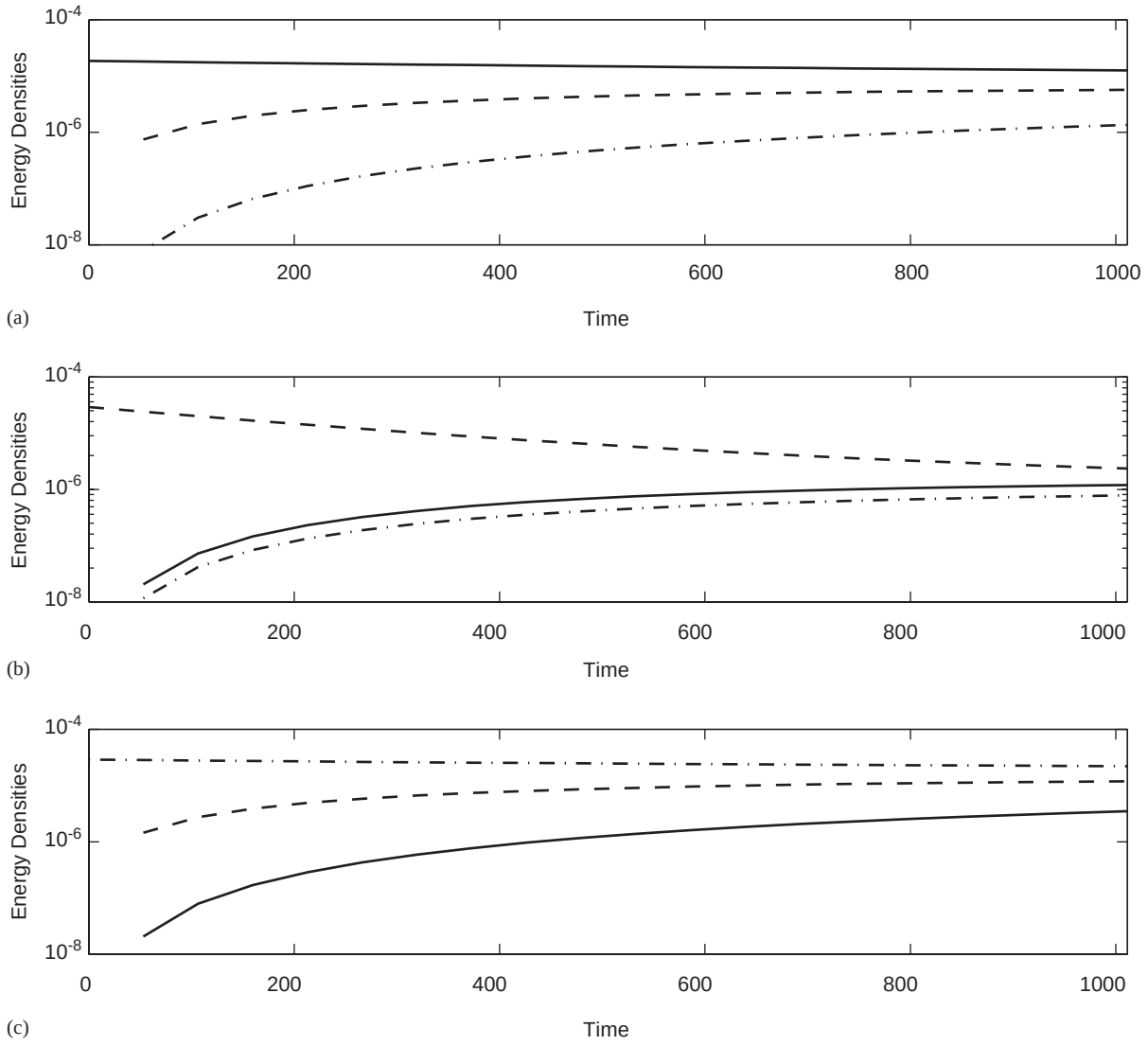

Fig. 7. The evolution of energy density in each of the three rooms for the period analyzed in Section 4. ————, response in room 1; – – – – – –, response in room 2; – · – · –, response in room 3. The eigenvalues are $\lambda_1 = 0$, $\lambda_2 = 4.7 \times 10^{-4}$, and $\lambda_3 = 22.5 \times 10^{-4}$. The eigenvectors are $\mathbf{v}^1 = \{2.9; 2.9; 2.9\} \times 10^{-3}$, $\mathbf{v}^2 = \{4.0; 0.47; -2.7\} \times 10^{-3}$, and $\mathbf{v}^3 = \{1.8; -5.8; 1.2\} \times 10^{-3}$. Total time considered was $\frac{1}{2}(1/\lambda_3)$: (a) a single source in room 1; (b) a single source in room 2; (c) a single source in room 3.

given that adding an extra receiver adds extra data to fit the parameters to. It must be noted, however, that the fit in the three room case is much more difficult overall than the fit in the two room case because the space that the fit algorithm must explore is much larger. Also, if higher noise amplitudes and/or less time is scrutinized, the fit fails to find the correct eigenvalues.

It is seen (Fig. 9) that the chi-square value is about unity for a sufficient number of receivers and sufficiently low noise. The value of chi-square is large (data points not plotted) when only a few

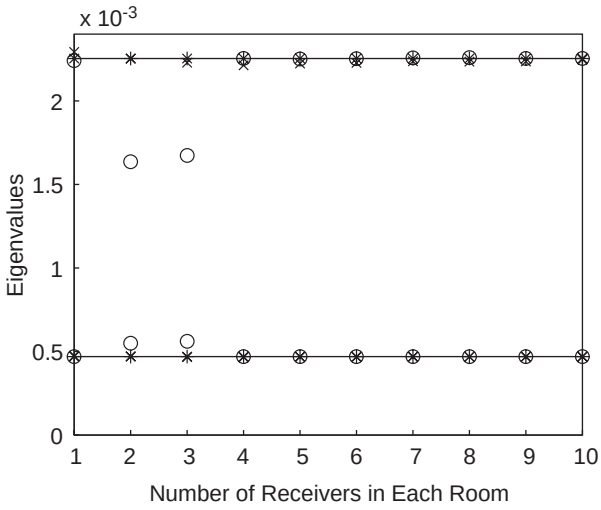

Fig. 8. The best fit to λ_2 and λ_3 for the three room system for various numbers of receivers in each room and noise levels. ————, correct value(s); ∗ ∗, $\sigma = 0\%$; ○ ○, $\sigma = 15\%$; × ×, $\sigma = 30\%$. The fit is good with enough receivers present. The algorithm does not work well with higher noise amplitudes and/or less time.

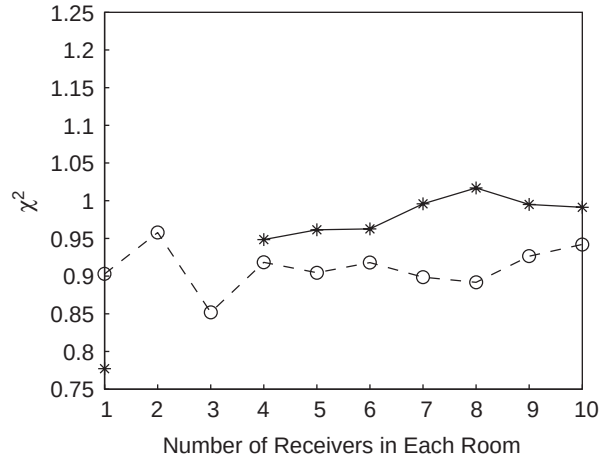

Fig. 9. The χ^2 value after the fit for various numbers of receivers and noise amplitudes. —∗—∗—, $\sigma = 15\%$; —○—○—, $\sigma = 30\%$. This value should fluctuate about unity. The large values of χ^2 for few receivers and low noise amplitude (omitted) reflect the lack of good fit. Other values close to unity show that the fit is good in the presence of a sufficient number of receivers.

receivers in each room are considered for the lower noise level. This indicates that the fit failed in those cases; a local, and wrong, minimum was found. The best fit to some of the data is plotted along with the data in Fig. 10.

The fitting algorithm in this three room case is successful, but not as robust as for the two room case. In particular, the large amount of time needed for a successful fit in the three room case is

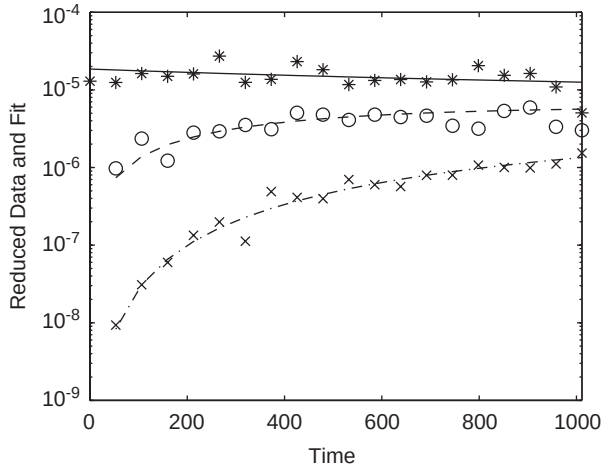

Fig. 10. An example of the actual fit to the data with noise fluctuations $\sigma = 30\%$. $* *$, data from a site in room 1; ————, fit to data from room 1; $\circ\ \circ$, data from a site in room 2; – – – – –, fit to data from room 2; $\times\ \times$, data from a site in room 3; – · – · –, fit to data from room 3. The source in room 1. The overall fit was to data from 10 receivers in each room.

disturbing. There is evidence, however, that the lack of robustness is due to the numerical fit algorithm, not the χ^2 formulation. The Newton algorithm finds *a* minimum of Eq. (25b), but does not necessarily find the global minimum. When better "first guesses" are used in the Newton algorithm for the eigenvalues and eigenvector element, the fit is successful even when data was examined only out to $t_{\max} = 210$. This suggests that another numerical minimization algorithm, such as a simplex method or simulated annealing [24] might be preferable.

It is noteworthy that accurate fits (and correct eigenvalues and eigenvectors) can be obtained when only short times are analyzed. This is promising for the ultimate application to DNS data for which long time calculations are expensive.

5. Conclusions and future work

The goal of this paper was to fit diffusion parameters to data which was unambiguously known to have underlying diffusive behavior. We have developed a procedure that is successful in fitting diffusion parameters in systems that admit to substructuring—long time behavior is predicted from analysis of only short time data—although the procedure does not inherently require the substructuring. The substructuring was exploited to simplify the nonlinear fit method used.

At least two immediate extensions are obvious: the extension to more substructures and the extension to no substructuring, i.e. fitting directly to the form of Eq. (9). Each of these generalizations would be straightforward, though they may well require a better, and more global, nonlinear fitting algorithm because of the large number of parameters that would need to be adjusted.

It is also necessary to apply these ideas to real DNS data, data for which the diffusion ansatz itself may be incorrect.

Acknowledgements

This work was supported by NSF grant CMS-0201346.

Appendix A. Generation of noise

In this section the procedure used to construct noise artificially is explained.

We begin by constructing centered Gaussian distributed noise with unity standard deviation using the *Box–Muller* method [24]. Consider a pair of uniformly distributed numbers $\xi_1, \xi_2 \in [0, 1]$. By performing the transformation

$$\eta_1 = \sqrt{-2 \ln \xi_1} \cos 2\pi\xi_2, \tag{27a}$$

$$\eta_2 = \sqrt{-2 \ln \xi_1} \sin 2\pi\xi_2, \tag{27b}$$

one obtains a pair of quantities η_1, η_2 with the normal (Gaussian) distribution

$$f(\eta) = \frac{1}{\sqrt{2\pi}} \mathrm{e}^{-\eta^2/2}. \tag{28}$$

That is, η_1, η_2 are two independent Gaussian distributed numbers with a mean of zero and standard deviation of unity.

Then, for each r and t, construct

$$\chi_{rt} = \frac{\sum_{i=1}^{n_\eta} \eta_i^2}{n_\eta}, \tag{29}$$

a chi-square distribution of positive random numbers with mean unity and standard deviation

$$\sigma = \sqrt{2/n_\eta}. \tag{30}$$

Therefore, the number of smoothing points n_η to be used in the construction of χ should be $2/\sigma^2$, and Eq. (30) defines σ. Finally, noisy data $\mathbf{G}$ is constructed by multiplying the original underlying smooth mean square response Ψ by this χ and a gain $\mathbf{g}$, i.e. $\mathbf{G}_r(t) = \mathbf{g}_{rn}\psi_n\chi_{rt}$.

Appendix B. Solution for the three room problem

The problem is, given $\mathbf{v}^1$, $\mathbf{h}$, and $\mathbf{v}_1^2$, solve for the remaining elements of $\mathbf{v}^2$ and $\mathbf{v}^3$ in

$$\mathbf{v}_1^1\mathbf{h}_1\mathbf{v}_1^2 + \mathbf{v}_2^1\mathbf{h}_2\mathbf{v}_2^2 + \mathbf{v}_3^1\mathbf{h}_3\mathbf{v}_3^2 = 0, \tag{31a}$$

$$\mathbf{v}_1^1\mathbf{h}_1\mathbf{v}_1^3 + \mathbf{v}_2^1\mathbf{h}_2\mathbf{v}_2^3 + \mathbf{v}_3^1\mathbf{h}_3\mathbf{v}_3^3 = 0, \tag{31b}$$

$$\mathbf{v}_1^2\mathbf{h}_1\mathbf{v}_1^3 + \mathbf{v}_2^2\mathbf{h}_2\mathbf{v}_2^3 + \mathbf{v}_3^2\mathbf{h}_3\mathbf{v}_3^3 = 0, \tag{31c}$$

$$\mathbf{v}_1^2\mathbf{h}_1\mathbf{v}_1^2 + \mathbf{v}_2^2\mathbf{h}_2\mathbf{v}_2^2 + \mathbf{v}_3^2\mathbf{h}_3\mathbf{v}_3^2 = 1, \tag{31d}$$

$$\mathbf{v}_1^3\mathbf{h}_1\mathbf{v}_1^3 + \mathbf{v}_2^3\mathbf{h}_2\mathbf{v}_2^3 + \mathbf{v}_3^3\mathbf{h}_3\mathbf{v}_3^3 = 1. \tag{31e}$$

Physically, we know the subspace that $\mathbf{v}^2$ and $\mathbf{v}^3$ span and mutual orthogonality, so there is only one free parameter (say, an angle) to completely specify the two higher eigenvectors. Mathematically, there are five remaining orthogonality conditions after $\mathbf{v}^1$ has been normalized and six elements of the other two higher eigenvectors, so one element must be specified in order to be able to solve for everything.

If we make the following definitions:

$$a = \mathbf{v}_2^1\mathbf{h}_2, \tag{32a}$$

$$b = \mathbf{v}_3^1\mathbf{h}_3, \tag{32b}$$

$$c = -\mathbf{v}_1^1\mathbf{h}_1\mathbf{v}_1^2, \tag{32c}$$

$$d = \mathbf{h}_2, \tag{32d}$$

$$e = \mathbf{h}_3, \tag{32e}$$

$$f = 1 - \mathbf{h}_1(\mathbf{v}_1^2)^2, \tag{32f}$$

then

$$\mathbf{v}_2^2 = \frac{ace/b^2 \pm \sqrt{(a^2c^2e^2/b^4) - (d + (a^2e/b^2))((c^2e/b^2) - f)}}{(d + (a^2e/b^2))}, \tag{33a}$$

$$\mathbf{v}_3^2 = -\frac{a}{b}\mathbf{v}_2^2 + \frac{c}{b}. \tag{33b}$$

The $\pm$ ambiguity in Eq. (33a) is a labeling issue. It is impossible to know *a priori* which of the higher eigenvectors is $\mathbf{v}^2$ and which is $\mathbf{v}^3$. In our implementation, the $+$ sign is taken.

Furthermore, if we define

$$\beta = \frac{-\mathbf{v}_2^2\mathbf{h}_2(\mathbf{v}_1^2\mathbf{v}_3^1\mathbf{h}_3 - \mathbf{v}_1^1\mathbf{v}_3^2\mathbf{h}_3) + \mathbf{v}_3^2\mathbf{h}_3(\mathbf{v}_1^2\mathbf{v}_2^1\mathbf{h}_2 - \mathbf{v}_1^1\mathbf{v}_2^2\mathbf{h}_2)}{\mathbf{v}_1^2\mathbf{h}_1}, \tag{34a}$$

$$\gamma = \mathbf{v}_1^2\mathbf{v}_3^1\mathbf{h}_3 - \mathbf{v}_1^1\mathbf{v}_3^2\mathbf{h}_3, \tag{34b}$$

$$\delta = -(\mathbf{v}_1^2\mathbf{v}_2^1\mathbf{h}_2 - \mathbf{v}_1^1\mathbf{v}_2^2\mathbf{h}_2), \tag{34c}$$

$$\alpha^2 = \beta^2\mathbf{h}_1 + \gamma^2\mathbf{h}_2 + \delta^2\mathbf{h}_3, \tag{34d}$$

then

$$\mathbf{v}_1^3 = \frac{\beta}{\alpha}, \tag{35a}$$

$$\mathbf{v}_2^3 = \frac{\gamma}{\alpha}, \tag{35b}$$

$$\mathbf{v}_3^3 = \frac{\delta}{\alpha}. \tag{35c}$$

Existence of a solution is governed by the discriminant in Eq. (33a). Depending on the values of $\mathbf{h}$ and $\mathbf{v}^1$, there may be a well defined upper bound on the magnitude of $\mathbf{v}_1^2$ in order for there to be a solution. Otherwise, $\mathbf{v}_1^2$ can be any non-zero number. In our implementation $\mathbf{v}_1^2$ is taken to be positive to enforce uniqueness of the solution.

References

[1] R.H. Lyon, R.G. DeJong, *Theory and Application of Statistical Energy Analysis*, second ed., Butterworth-Heimann, London, 1995.
[2] E.H. Dowell, Yuji Kubota, Asymptotic modal analysis and SEA of dynamical systems, *Journal of Applied Mechanics* 52 (1995) 949–957.
[3] C.H. Hodges, J. Woodhouse, Theories of noise and vibration transmission in complex structures, *Reports on Progress in Physics* 49 (1986) 107–170.
[4] J. Woodhouse, An approach to the theoretical background of SEA applied to structural vibration, *Journal of the Acoustical Society of America* 69 (1981) 1695–1709.
[5] B.R. Mace, P.J. Shorter, Energy flow models from finite element analysis, *Journal of Sound and Vibration* 233 (2000) 369–389.
[6] C. Simmons, Structure-borne sound transmission through plate junctions and estimates of SEA coupling loss factors using the FEM method, *Journal of Sound and Vibration* 144 (1991) 215–227.
[7] J.A. Steel, R.J. Craik, Statistical energy analysis of structure-borne sound transmission by FEM, *Journal of Sound and Vibration* 178 (1993) 553–561.
[8] K. Shankar, A.J. Keane, A study of the vibrational energies of two coupled beams by FEM and receptance methods, *Journal of Sound and Vibration* 181 (1995) 801–838.
[9] C.R. Fredo, SEA-like approach for the derivation of energy flow coefficients with a finite element model, *Journal of Sound and Vibration* 199 (1997) 645–666.
[10] M.L. Lai, A. Soom, Prediction of transient vibration envelopes using SEA techniques, *Journal of Vibration and Acoustics* 122 (1990) 127–137.
[11] R.J. Pinnington, D. Lednik, Transient SEA of an impulsively excited two oscillator system, *Journal of Sound and Vibration* 189 (1996) 249–264.
[12] R.S. Langley, P.G. Bremner, A hybrid method for the vibrational analysis of complex structural-acoustic systems, *Journal of the Acoustical Society of America* 105 (1999) 1657–1671.
[13] R.L. Weaver, Equipartition and mean-square responses in large undamped structures, *Journal of the Acoustical Society of America* 110 (2) (2001) 894–903.
[14] J.W. Gregory, R.F. Keltie, SEA system identification using transient vibration data, in: *Proceedings of the Second International AutoSEA Users Conference*, Detroit-Troy Marriott—Troy, Michigan, USA, 2002.
[15] A. Tourin, A. Derode, A. Peyre, M. Fink, Transport parameters for an ultrasonic pulsed wave propagating in a multiple scattering medium, *Journal of the Acoustical Society of America* 108 (2) (2000) 503–512.
[16] R.L. Weaver, Diffusivity of ultrasound in polycrystals, *Journal of the Mechanics and Physics of Solids* 38 (1) (1990) 55–86.
[17] D.E. Newland, *An Introduction to Random Vibrations and Spectral Analysis*, second ed., Longman House, 1984.
[18] R.L. Weaver, Spectral statistics in elastodynamics, *Journal of the Acoustical Society of America* 85 (3) (1989) 1005–1013.
[19] R.L. Weaver, On the ensemble variance of reverberation room transmission function, the effect of spectral rigidity, *Journal of Sound and Vibration* 130 (3) (1989) 487–491.
[20] O.I. Lobkis, R.L. Weaver, I. Rozhkov, Power variances and decay curvature in a reverberant system, *Journal of Sound and Vibration* 237 (2) (2000) 281–302.

[21] C. Kittel, H. Kroemer, *Thermal Physics*, second ed., W.H. Freeman and Company, New York, 1980.
[22] The MathWorks, Inc., Natick, MA 01760-2098, *Optimization Toolbox for Use with MATLAB*, *User's Guide*, 1990–2004.
[23] Jer-Nan Juang, R.S. Pappa, An eigensystem realization algorithm for modal parameter identification and model reduction, *Journal of Guidance* 8 (5) (1985) 620–627.
[24] W.H. Press, S.A. Teukolsky, W.T. Vetterling, B.P. Flannery, *Numerical Recipes: The Art of Scientific Computing*, second ed., Cambridge University Press, Cambridge, 1992.